

Fixed-point numerical-reconstruction for digital holographic microscopy

Nitesh Pandey and Bryan Hennelly*

Department of Computer Science, National University of Ireland, Maynooth Maynooth, Co. Kildare, Ireland

*Corresponding author: bryanh@cs.nuim.ie

Received December 15, 2009; revised February 23, 2010; accepted February 25, 2010; posted March 2, 2010 (Doc. ID 121579); published March 31, 2010

In this Letter, we study the reconstruction of digital holograms of microscopic objects using a fixed-point representation of the numerical-reconstruction process. For different bit levels in our fixed-point reconstruction algorithm, we investigate the errors introduced to both the reconstructed image intensity and the unwrapped quantitative phase information. Experimental results based on a microscopic lens array are provided. © 2010 Optical Society of America

OCIS codes: 090.1995, 200.3050, 100.5088.

Digital holographic microscopy (DHM) is a quantitative phase contrast imaging technique with a number of important properties, such as numerical aberration compensation [1] and numerical refocusing [2]. It is suitable for high-resolution label-free analysis of living cells [3], for investigations on reflective surfaces such as microelectromechanical systems [4] as well as surface profiling with nanometer accuracy. To the best of our knowledge, the numerical-reconstruction process that is used both in industry and in the research community employs floating-point arithmetic. This Letter addresses the numerical-reconstruction of digital holograms using fixed-point integer arithmetic. We investigate the advantages of such an approach as well as the errors introduced into the quantitative phase.

There are two major formats for representing real numbers in bit-sequences of 0s and 1s; floating point and fixed point. Computationally fixed-point arithmetic is less demanding than floating-point arithmetic. Fixed-point devices have a simpler architecture with fewer gates and transistors and thus have smaller cycle clock time and are faster. Additionally fixed-point processors consume less power and generate less heat than floating-point processors and are thus well suited to portable devices where battery life is important. Many embedded systems and handheld units have fixed-point processors. Already there are variants of DHM that do entail some degree of portability in the recording side such as submersible-digital inline microscopes for detection of life forms in remote inaccessible areas [5], holographic on-chip cytometry [6], plankton sampling [7], etc. In scenarios such as these, it is essential to optimize the numerical-reconstruction process so that it uses up as little resources as possible if reconstruction is to be carried out on site.

A floating-point bit sequence in binary can be broken into two smaller bit sequences, the signed mantissa and the signed exponent. In the Institute of Electrical and Electronics Engineers floating-point notation [8] a number is represented by $N = (-1)^s \times m \times 2^{(e-127)}$ where s is the sign bit, m is the standard binary number represented by the (normalized) fractional mantissa, and e is the (biased) exponent.

Employing a mantissa and an exponent allows the radix point to “float” and thus allows calculations over a wide range of magnitudes. Fixed-point notation on the other hand is simpler. The most common fixed-point notation is the “two’s complement.” In two’s complement, the leading bit of positive numbers is 0 and of negative numbers is 1. The value represented is obtained by assuming that the leftmost bit is negative and then calculating the binary value of the number. The spacing between all the numbers is uniform, and thus fixed-point notation can be viewed simply as a scaled integer. The position of the radix point is fixed. A thorough description of fixed- and floating-point arithmetic can be found in [9].

The setup for a typical DHM is shown in Fig. 1. In this study we present an algorithm for Fresnel propagation of complex phase data for phase contrast mi-

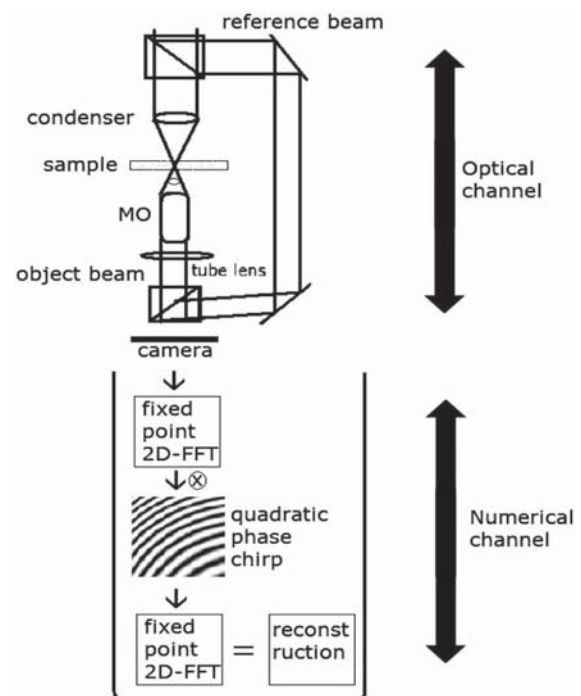


Fig. 1. Setup for DHM. The optical and the numerical channel in digital holographic imaging are shown.

croscopy that is entirely based on fixed-point arithmetic. In addition, we test our fixed-point algorithm on experimentally recorded digital holograms of a microlens array. We investigate the quality of the phase reconstructions and determine the minimum number of bits that give good reconstruction of the quantitative phase. Previous studies on quantization have focused on reducing the number of bits only in the digital hologram for compression [10,11]. By limiting the number of bits for every stage in the reconstruction algorithm we are effectively quantizing all the variables in the reconstruction channel. In our experiments, we use a commercially available DHM-T1000 from LynceeTec Inc. Using this microscope, the hologram of a microlens is recorded. An off axis architecture is employed and the hologram is captured with a microscope objective of power 10 \times and NA 0.25. The camera in this microscope is a 1392 \times 1040 pixels fire wire camera, and the laser is a monochromatic 682.5 nm laser source. Numerous algorithms exist that simulate the Fresnel transform [12]. These different algorithms are derived from different expressions for the Fresnel Transform. For example, by expressing the Fresnel transform as a chirp multiplication followed by a Fourier transform followed by a chirp multiplication we may derive the direct method algorithm. This uses a single fast Fourier transform (FFT) algorithm. By expressing the Fresnel transform as a chirp multiplication in the Fourier domain we may arrive at the convolution or spectral method. This is composed of two FFT algorithms and in general is the preferred algorithm used industrially. This is because the output sampling interval is equal to the CCD pixel pitch, and this is true regardless of the distance parameter. We limit our study to the fixed-point implementation of the spectral method to reconstruct microscopic specimens. We use MATLAB's fixed-point toolbox in our experiments.

The key step in this implementation is the 2D fixed-point FFT algorithm. For this study we employ an "in-place" radix-2 fixed-point FFT algorithm as described in [13]. All the variables involved in all the stages of the reconstruction process (the phase hologram, the FFT twiddle factors and the quadratic chirp matrix elements) are essentially sines and cosines (fractions lying between -1 and 1). They can be represented by choosing n bits, where one bit is assigned to the sign of the number and the remaining $n-1$ bits are assigned to representing the fractional part. Sines and cosines are calculated by the Taylor series expansion in fixed-point processors. This is computationally expensive as each element requires many multiplications and additions and can be speeded up using a precalculated table [14]. For this reason almost all DSP systems employ a precalculated table of sines called the look up table (LUT). The fixed-point reconstruction algorithm is as follows:

- Convert discrete phase signal P into the chosen fixed-point notation of n bits.
- Perform discrete 2D fixed-point FFT of P . $A = \text{fixedptfft2}(P)$.

- Calculate grid of the X - Y plane. $(m, n) = (m\Delta x, n\Delta y)$ for $m = -\frac{M}{2}$ to $\frac{M}{2}-1$ and $n = -\frac{N}{2}$ to $\frac{N}{2}-1$.
- Calculate $B = e^{i2\pi\lambda d} e^{-i\pi\lambda d(m/Mdy)^2 + (n/Ndx)^2}$ in fixed-point precision using a look up table where λ is the wavelength, d is the specimen distance, dy and dx are the pixel pitches of the sensor.
- Convert B into the chosen fixed-point notation of n bits.
- Calculate $C = A * B$.
- Perform discrete 2D fixed-point FFT of C . $D = \text{fixedptfft2}(C)$.

To compare the efficiency of the fixed-point reconstructions with that of the floating-point reconstructions, the reconstructed phase is unwrapped using the discrete cosine transform method [15]. The phase reconstruction becomes perceptible after 18 bits of representing data, and the shape of the microlens is completely perceptible at 20 bits [Fig. 2(a)]. The rms error in the surface height at 20 bits is 140 nm. At 24 bits it is 6.28 nm [Fig. 2(b)], and at 32 bits it is 0.028 nm. While the fixed-point arithmetic-based reconstruction algorithm has the disadvantage of introducing some error into the quantitative phase measurements, it takes up less computational resources when compared to floating-point arithmetic. The time taken by a version implemented on hardware is dependent on the total number of computations involved in the algorithm, which can be calculated approximately. The total number of operational cycles required for multiplying a p bit word with a q bit word is pq , and the total number of operational cycles required for the addition of a p bit word to a q bit word is $\max(p, q)$ [16]. A radix-2 FFT takes $2N \log N$ multiplications and $3N \log N$ additions [13]. We assume that all the variables (including the hologram samples) in the numerical-reconstruction process

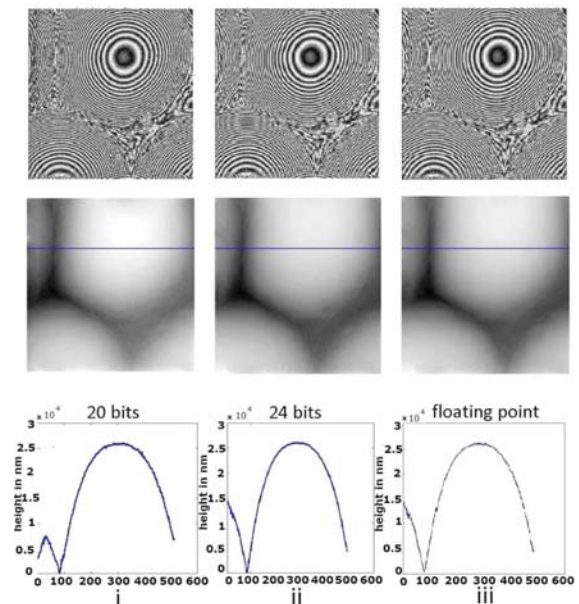


Fig. 2. (Color online) Reconstructions for (a) 20 bits fixed point, (b) 24 bits fixed point, and (c) 64 bit (double precision) floating point. The surface profiles (third row) are shown for the horizontal black line in the second row.

have b bits. For a hologram of size N pixels, element-wise multiplication of a N -pixel chirp matrix with the output from a N -pixel FFT matrix requires $\sim O(Nb^2)$ multiplications. Therefore, the total computational cycles required for reconstruction (two FFTs and one chirp multiplication) will be $b^2(4N \log N + N) + b(6N \log N)$. The number of computational cycles and the resulting error in the measurement of surface height of a microlens for a 512×512 hologram is shown in Fig. 3. The latter is calculated by comparing the unwrapped phase from reconstructions from the fixed-point algorithm against “ideal” reconstruction from the floating-point algorithm. The * line shows the increase in the number of computations in the reconstruction algorithm as the variable bit length. The x line shows the corresponding decrease in the rms error of the unwrapped phase. It is seen that as the bit size increases, the number of computations grows almost linearly ($N \log N$ complexity), but the error in the reconstructed phase decreases exponentially ($\frac{1}{2^N}$). At 24 bits the total number of operations is approximately 50% less than those at 32 bits.

We have reconstructed phase contrast digital holograms using fixed-point arithmetic for the numerical-reconstruction process. We have shown that it is possible to reconstruct quantitative phase data with good fidelity using fixed-point arithmetic with 20 bits or more. The number of computations decrease with

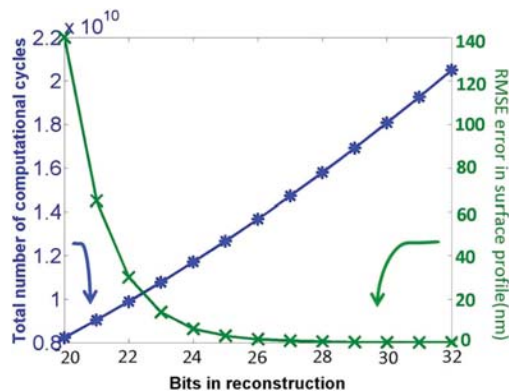


Fig. 3. (Color online) Number of computations required in reconstruction and the rms error in the surface profile. Experimental results show that each additional bit reduces the error by half.

the number of bits, but the error in the signal increases. The number of bits can be chosen to suit the accuracy required by the application. We believe that this work will facilitate the use of low-power fixed-point processors for a fully portable record display DHM. Such a device may have widespread application in on site industrial inspection and bedside cellular imaging.

The research leading to these results has received funding from the European Community's Seventh Framework Programme FP7/2007–2013 under grant agreement no. 216105 and also Science Foundation Ireland under the National Development Plan.

References

1. A. Stadelmaier and J. H. Massig, *Opt. Lett.* **25**, 1630 (2000).
2. F. Dubois, C. Schockaert, N. Callens, and C. Yourasowsky, *Opt. Express* **14**, 5895 (2006).
3. D. Carl, B. Kemper, G. Wernicke, and G. V. Bally, *Appl. Opt.* **43**, 6536 (2004).
4. G. Coppola, P. Ferraro, M. Iodice, S. D. Nicola, A. Finizio, and S. Grilli, *Meas. Sci. Technol.* **15**, 529 (2004).
5. S. K. Jericho, J. Garcia-Sucerquia, W. Xu, M. H. Jericho, and H. J. Kreuzer, *Rev. Sci. Instrum.* **77**, 043706 (2006).
6. S. Seo, T. W. Su, D. K. Tseng, A. Erlinger, and A. Ozcan, *Lab Chip* **9**, 777 (2009).
7. Peter R. Hobson and John Watson, *J. Opt. A* **4**, S34 (2002).
8. "IEEE Standard for Floating-Point Arithmetic," *IEEE Std 754–2008*, pp. 1–58, (2008).
9. B. Parhami, *Computer Arithmetic, Algorithms and Hardware Designs* (Oxford U. Press, 2000).
10. A. E. Shortt, T. J. Naughton, and B. Javidi, *Opt. Express* **14**, 5129 (2006).
11. G. A. Mills and I. Yamaguchi, *Appl. Opt.* **44**, 1216 (2005).
12. B. M. Hennelly and J. T. Sheridan, *J. Opt. Soc. Am. A Opt. Image Sci. Vis* **22**, 917 (2005).
13. C. Van Loan, *Computational Frameworks for the Fast Fourier Transform* (SIAM, 1992).
14. N. Pandey, D. P. Kelly, T. J. Naughton, and B. M. Hennelly, *Proc. SPIE* **7442**, 744205 (2009).
15. D. Kerr, G. H. Kaufmann, and G. E. Galizzi, *Appl. Opt.* **35**, 810 (1996).
16. A. Aho, J. Hopcroft, and J. Ullman, *Design and Analysis of Computer Algorithms* (Addison-Wesley, 1974).